Organic & Biomolecular Chemistry

Accepted Manuscript

ROYAL SOCIETY OF CHEMISTRY

www.rsc.org/obc

Journal Name

RSCPublishing

COMMUNICATION

Helical peptaibol mimics are better ionophores when racemic than when enantiopure

Cite this: DOI: 10.1039/x0xx00000x

Sarah J. Pike,[‡,a,b] Jennifer E. Jones,[‡,a,b] James Raftery,[a] Jonathan Clayden,[a]* and Simon J. Webb[a,b]*

Received 00th January 2012,
Accepted 00th January 2012

DOI: 10.1039/x0xx00000x

www.rsc.org/

Helical peptide foldamers rich in α-aminoisobutyric acid (Aib) act as peptaibol-mimicking ionophores in the phospholipid bilayers of artificial vesicles. Racemic samples of these foldamers are more active than their enantiopure counterparts, which was attributed to differing propensities to form aggregates with crystal-like features in the bilayer.

Peptide foldamers containing high proportions of the achiral quaternary residue α-aminoisobutyric acid (Aib) are of keen interest because of their close relationship to peptaibols, a class of antimicrobial peptides (AMPs) produced by *Trichoderma* fungi. Peptaibols are thought to exert their antibiotic activity by permeabilising the membranes of bacteria,[1] with the most studied example being 19-residue alamethicin. This ionophoric activity is frequently rationalised using "barrel-stave" channel models, the formation of which requires aggregation of membrane-spanning peptaibols in lipid bilayers.[2] Nonetheless, the trichogins, including 6-residue trichodecenin I and 4-residue peptaibolin are membrane-active, despite being too short to span bilayers.[3] Aggregation is thought to be crucial for the activity of short AMPs, either during "carpet-like" aggregation of cationic peptides on the surface (the Shai-Matsuzaki-Huang mechanism[4]) or during membrane-thinning "barrel-stave" aggregation, as suggested for 10-residue trichogin GA IV.[5] Similarly, peptide aggregation on or in cell membranes is proposed to be important in Alzheimer's disease[6] and type II diabetes,[7] where amyloid accumulation induces cell death.[8] Cell death has been attributed to toxic amyloid oligomers causing a loss of cell membrane integrity, which occurs *via* mechanisms related to those followed by AMPs, with ill-defined oligomers causing pore formation and nonspecific membrane permeabilisation.[9] However an amyloid-like mechanism for membrane activity has not yet been associated with peptaibols.

Peptide foldamers composed exclusively of Aib residues adopt stable 3_{10} helical conformations[10] (Figure 1), a conformation found within some peptaibols.[11] Aib oligomers composed only of achiral monomers cannot have a screw-sense preference and comprise equal populations of rapidly interconverting *M* and *P* helices.[12] The introduction of a single chiral amino acid at the N- or C-terminus can bias the population distribution towards one helical conformation.[13]

Several peptaibols (e.g. the cephaibols) carry an N-terminal L-phenylalanine (Phe) residue that appears to play a role in promoting conformational mobility in an adjacent run of Aib residues.[14] In an investigation of the effect of N-terminal chiral residues on the aggregation of related artificial 3_{10}-helical Aib foldamers, we found that the self-association of Aib oligomers in $CDCl_3$, a low-polarity solvent that mimics the centre of a lipid bilayer, was enhanced by an N-terminal carboxybenzyl (Cbz) protected Phe residue.[15] Recently we also found that synthetic Aib foldamers can show peptaibol-like membrane activity, with long achiral foldamers forming discrete ion channels but shorter homologues destabilising bilayers.[16] Since the membrane activity of peptaibols depends on aggregation, we wondered if comparing the activity of racemic and homochiral samples of Aib-rich foldamers would allow the effect of differing inter-foldamer interactions on membrane activity to be examined in isolation from other changes in foldamer structure.

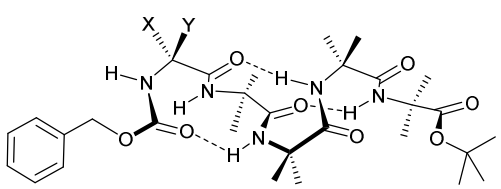

(*S*)-**1** (X = H, Y = CH_2Ph) (*S*)-**2** (X = CH_3, Y = $CH(CH_3)_2$)

(*rac*)-**1** (X, Y = H, CH_2Ph) (*rac*)-**2** (X, Y = CH_3, $CH(CH_3)_2$)

Figure 1. Foldamers bearing either N-terminal (*S*)-phenylalanine (Cbz-L-PheAib$_4$O^{t}Bu, **1**, X = H; Y = Bn) or N-terminal (*S*)-(α)-methylvaline (Cbz-L-MeValAib$_4$O^{t}Bu, **2**, X = Me; Y = *i*-Pr), shown in a 3_{10} helical conformation.

Here we report that the membrane activities of enantiopure foldamers **(*S*)-1** and **(*S*)-2** are markedly different from their corresponding racemic mixtures, **(*rac*)-1** and **(*rac*)-2** (Figure 1). Inter-peptide interactions were assessed using ^{1}H NMR spectroscopy and X-ray crystallography, with membrane activity quantified by ion transport and dye release studies in artificial phospholipid vesicles.

The (*R*) and (*S*) enantiomers of each Aib oligomer **1** and **2**, bearing Cbz-protected Phe or the quaternary amino acid α-methylvaline (MeVal) at the N-termini (Figure 1), were prepared by literature procedures.[13a,13b,14,17] The racemic mixtures were obtained by dissolving equal amounts of the enantiomers then removing the solvent under reduced pressure.

Both **1** and **2** contained four Aib residues to ensure folding into a 3_{10} helix, which was confirmed by DMSO-d_6 titrations (see ESI).[15] Strong self-association of peptaibols in non-polar environments has been suggested to increase the tendency of these compounds to form self-assembled channels.[15,18] To model how these folded peptides might self-associate in a bilayer, changes in their ^{1}H NMR spectra were monitored as concentrated solutions in the apolar solvent $CDCl_3$ were progressively diluted.[19] However the concentration range studied for racemates **(*rac*)-1** and **(*rac*)-2** was limited by their lower solubility, as they had saturation concentrations (30 and 15 mM respectively) that were markedly lower than their enantiopure counterparts (150 and 75 mM respectively, e.g. see Figure 2a). Both **(*rac*)-1** and **(*rac*)-2** also had melting points 24-35 °C higher than the enantiopure compounds (see the ESI). This combination of lower solubility and higher melting point suggests **(*rac*)-1** and **(*rac*)-2** are true racemates in the solid-state rather than conglomerates.[20]

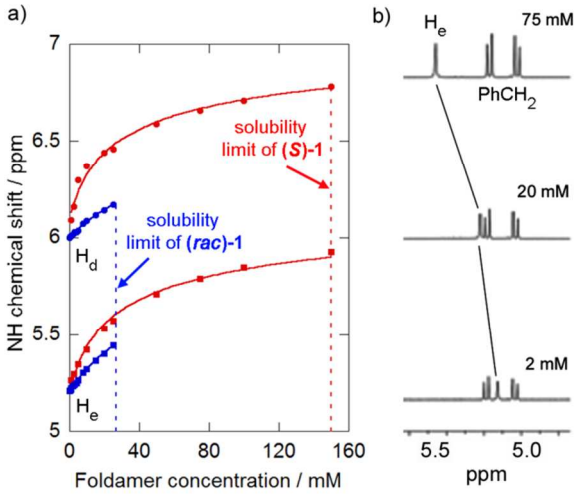

Figure 2. a) Changes in chemical shift of protons NH_d and NH_e of **(*S*)-1** (500 MHz, 298 K, $CDCl_3$) upon dilution (red, curve fit for K = 19 M^{-1} and **(*rac*)-1** (blue, curve fit for K = 5 M^{-1}). b) Partial ^{1}H NMR stack plot of **(*S*)-2** (500 MHz, 298 K, $CDCl_3$) at 75 mM, 20 mM and 2 mM showing change in chemical shift of NH_e. The NH resonances of **1** and **(*S*)-2** were labelled alphabetically from low to high field.

Foldamer **(*S*)-1** showed substantial changes ($\Delta\delta$ > 0.6 ppm) in the chemical shifts of the NH signals of the Phe residue (NH_e) and the first Aib residue at the N-terminus (NH_d, NH resonances labelled alphabetically from low to high field) on dilution from 150 mM to 1 mM whilst **(*S*)-2** showed a ~0.35 ppm change for one NH resonance (H_e, the NH of either the MeVal or first Aib, see ESI) on dilution from 75 mM to 2 mM (Figure 2b). Similar studies on **(*rac*)-1** and **(*rac*)-2** revealed analogous yet smaller changes in the chemical shifts of the same protons. The resonance of the easily identified N-terminal NH (NH_e) in **(*S* or *rac*)-1** was the most sensitive to changes in the concentration of these compounds, consistent with head-to-tail (N-terminus to C-terminus) aggregation in solution.[15,21] The changes in chemical shift fitted a dimerisation model[15] and dimerisation constants were calculated for each compound by standard iterative curve fitting to give $K = 19 \pm 9$ M^{-1} for **(*S*)-1**, $K = 5 \pm 1$ M^{-1} for **(*rac*)-1** and $K < 4$ M^{-1} for both **(*S*)-2** and **(*rac*)-2**. The values for **(*S*)-1** were consistent with previously reported values,[15] whereas the values for **(*S*)-2** clearly show the Cbz-L-MeVal group weakens dimerisation compared to Cbz-L-Phe. Surprisingly **(*rac*)-1** appeared to dimerise more weakly than **(*S*)-1** despite its markedly lower solubility.

The lower solubility of the racemates allowed crystals suitable for X-ray crystallography to be obtained for **(*rac*)-1** (described previously[22]) and **(*rac*)-2**; conditions to crystallise the enantiopure analogues were not found. Indeed, Huc and co-workers have used this increased propensity of racemic mixtures to crystallise to elucidate the structure of helical aromatic oligoamide foldamers.[23] Both compounds crystallised in centrosymmetric space groups with *M* and *P* screw-sense conformers in the unit cell.[21] Both adopt 3_{10} helical structures with three $i \rightarrow i+3$ intramolecular hydrogen bonds producing a series of Type-III β-turns terminated by a Schellman-like motif at the C-terminal ester group.[24]

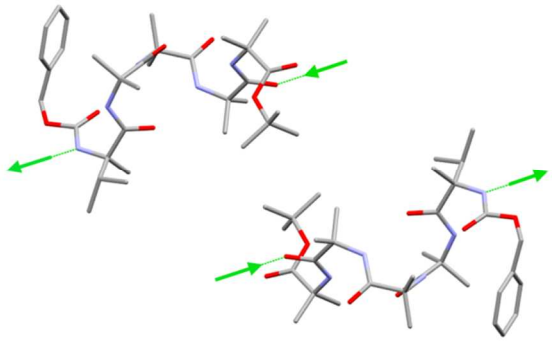

Figure 3. Side view of **(*rac*)-2** in the solid state showing side-by-side interactions between foldamers of opposite helicity. Intermolecular hydrogen bonds (green arrows, direction NH to C=O) connect oligomers of the same helicity into columns. See the ESI for all hydrogen bonds and the extended structure. Carbon atoms in grey, oxygen atoms in red, nitrogen atoms in light blue. Hydrogen atoms and molecules of solvation have been removed for clarity.

The crystal packing of **(*rac*)-2** shows intermolecular head-to-tail hydrogen bonds between helices of the same screw sense, involving the MeVal residue NH proton and an amide carbonyl of an adjacent foldamer (Figure 3). Oligomers of opposite screw-sense do not hydrogen bond with each other. The intermolecular hydrogen bonds continue the intramolecular hydrogen bonding pattern in the 3_{10} helices and reinforce the foldamer macrodipoles, leading to columns of foldamers with the same screw sense. Columns of opposite screw sense interact in a side-by-side antiparallel fashion. The crystal structure of **(*rac*)-1** was analogous,[22] with columns of oligomers of the same screw sense linked by intermolecular head-to-tail hydrogen bonds, but with intermolecular π-π interactions between antiparallel columns.[25]

To assess the ability of **(*S*)-1**, **(*rac*)-1**, **(*S*)-2** and **(*rac*)-2** to transport small ions through bilayers, we chose the phospholipid vesicle-based 8-hydroxypyrenetrisulfonate (HPTS) assay, using EYPC/cholesterol (4:1) vesicles with an interior pH of 7.4 and an exterior pH of 8.4.[26] After addition of

the ionophore, an external aliquot of NaOH (the base pulse) was added after 180 s to initiate transport. Addition of Triton X-100 after 45 minutes completely discharged the pH gradient and allowed normalisation of the data.

Initially Phe-capped foldamer **1** was assayed for its ability to allow ions to cross a bilayer. Addition of an aliquot of **(*S*)-1** solution (20 μL of 6 mM stock in MeOH) to EYPC/cholesterol vesicles (0.762 mM lipid) to give a membrane loading of 7.9 mol % (60 μM) produced an immediate change in fluorescence that suggested Na^+/H^+ antiport or Na^+/OH^- symport across the bilayer.[26,27] However the analogous experiment with **(*rac*)-1** at 60 μM showed significantly higher activity, with 75% greater discharge of the transmembrane ion gradient after 600 s. This higher ionophoric activity of the racemic solution was consistent across foldamer concentrations from 10 to 100 μM (see ESI[16]). Calculation of the fractional activities (*Y*) at each concentration after 1620 s using the method of Matile and co-workers[27] (Figure 4b) indicated that the racemic mixture had an EC_{50} of 11 μM, threefold lower than the enantiopure peptide (EC_{50} of 34 μM). This enhanced activity of the racemic mixture was also observed for the MeVal-capped foldamer, with discharge of the transmembrane ion gradient being 50% greater for **(*rac*)-2** than **(*S*)-2** after 600 s. The corresponding EC_{50} values were calculated as 5 and 20 μM respectively (Figure 4d).

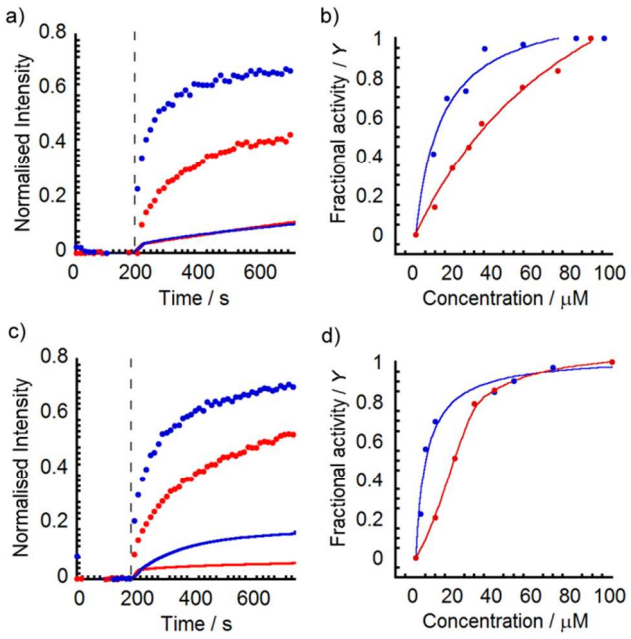

Figure 4. HPTS assay (filled circles) and 5/6-CF assay (solid lines) data for: (a) 60 μM **(*S*)-1** (red) and **(*rac*)-1** (blue); (c) 100 μM of **(*S*)-2** (red) and **(*rac*)-2** (blue). Fractional activities (Y) at 1620 s for (b) **(*S*)-1** (red) and **(*rac*)-1** (blue); (d) **(*S*)-2** (red) and **(*rac*)-2** (blue). Curve fits to guide the eye, dotted lines show base pulse.

It has been suggested that other short Aib oligomers compromise membranes by forming large pores,[3a] which can be assessed through the release of the dye 5/6-carboxyfluorescein (5/6-CF). Pores with a diameter of >30 Å would allow the passage of 5/6-CF though the membrane,[28] revealed by a large increase in fluorescence through the alleviation of self-quenching. As in the HPTS assay, EYPC/cholesterol (4:1) vesicles were employed but in this case containing 5/6-CF (50 mM). Addition of either **(*S*)-1**, **(*rac*)-1**, **(*S*)-2** or **(*rac*)-2** at concentrations from 10 to 100 μM to these dye-containing vesicles resulted in a slow increase in fluorescence at 517 nm (λ_{ex} 492 nm), indicative of dye leakage through pores without significant membrane disruption. This activity was generally higher for the racemic mixtures than for the enantiopure samples, and the Phe-capped foldamers were more active than MeVal-capped foldamers. Comparison of the data (normalised by TX-100 addition, Figure 4) to the HPTS data suggests that some of the membrane activity of these peptides does not arise from the formation of large pores/voids in the membrane.[29,30]

The lack of correlation between the membrane activity of these foldamers and dimerisation strength in $CDCl_3$ implies that dimerisation constants may not accurately predict the ionophoric activity of peptaibol mimics. Furthermore the observation that higher ionophoric activity instead correlates with lower solubility suggests a crystallisation-like mechanism for membrane permeabilisation by these foldamers, as distinct from head-to-tail dimerisation into discrete membrane spanning structures.[15,21] Such a mechanism might involve intra-membrane aggregates with structural elements in common with the packing geometries found in the crystal structure, with side-by-side interactions crucial for ionophoric activity.

"Carpet", "barrel-stave" or "amyloid", structures are often invoked in mechanisms of ionophoric activity by peptides. "Carpet" structures on the membrane surface that weaken the bilayer are often formed by cationic and hydrophilic peptides, such as PMAP-23, whereas a "barrel-stave" mechanism is more consistent with neutral and hydrophobic peptides, such as the peptaibol trichogin GA IV.[5b] The "amyloid" mechanism is less well understood, but membrane activity is proposed to stem from a heterogeneous population of aggregates that can both give channels and weaken the membrane.[9,31] Although, like trichogin GA IV, both **1** and **2** are very hydrophobic (clogP of 10.77 and 10.80 respectively, see the ESI) they are much shorter than this peptide and shorter even than a single phospholipid, effectively ruling out analogous behaviour. We therefore suggest an "amyloid"-type mechanism where heterogenous populations of membrane spanning aggregates are formed.[27] Initial partitioning of these hydrophobic foldamers into the membrane gives high effective concentrations, e.g. 5 mol % peptide corresponds to 50 mM in the bilayer, lying above the solubility limit for the racemates in $CDCl_3$.[32] Partitioning is followed by formation of solid state-like aggregates, with columns of foldamers of the same screw sense interacting with columns of opposite screw sense through side-by-side interactions; it is these side-by-side interactions that are stronger for the racemates. These columnar aggregates could produce a variety of membrane porating and/or membrane weakening structures with toroidal features. Some of these columnar aggregates permit the passage of large ions, like 5/6-CF, with some only allowing the passage of smaller ions.

The formation of ill-defined aggregates with crystal-like features that, like amyloid, both weaken bilayers and form channels may be an under-appreciated contribution to the membrane activity and cell toxicity of short Aib-containing peptides. Furthermore the administration of racemates of peptide-based synthetic ion channels and natural AMPs may provide a boost to membrane activity. Our work is also an indication of the exciting potential applications of synthetic foldamers in chemical biology. For example, responsive antibiotics may be accessible, with non-covalent recognition of a chemical trigger switching Aib foldamers between chiral and non-chiral conformations, thereby changing ionophoric ability.

We gratefully acknowledge Dr. J. Sanderson for the "NMR dilution fit" Excel spreadsheet used for dimerisation constant determination. We also thank Dr. S. Cockroft for his assistance

with preliminary PBC measurements.[29] This work was supported by the BBSRC (grant ref. I007962), ESPRC (grant ref. EP/K039547) and the ERC (Advanced Grant ROCOCO).

Notes and references

[a] School of Chemistry, University of Manchester, Oxford Road, Manchester, M13 9PL, UK. E-mail: clayden@man.ac.uk.
[b] Manchester Institute of Biotechnology, University of Manchester, 131 Princess St., Manchester, M1 7DN, UK. E-mail: S.Webb@manchester.ac.uk
‡ These authors contributed equally to this work.

Electronic Supplementary Information (ESI) available: NMR spectra, crystallographic data and dimerisation constant calculations. For ESI and crystallographic data in CIF or other electronic format (CCDC deposition number for **(*rac*)-2**: 1062574) see DOI: 10.1039/c000000x.

1. W. C. Wimley, *ACS Chem. Biol*. 2010, **5**, 905–917.
2. (a) S. Futaki, D. Noshiro, T. Kiwada and K. Asami, *Acc. Chem. Res*, 2013, **46**, 2924-2933; (b) D. S. Cafiso, *Annu. Rev. Biophys. Biomol. Struct*. 1994, **23**, 141-165.
3. (a) S. Bobone, Y. Gerelli, M. De Zotti, G. Bocchinfuso, A. Farrotti, B. Orioni, F. Sebastiani, E. Latter, J. Penfold, R. Senesie, F. Formaggio, A. Palleschi, C. Toniolo, G. Fragneto and L. Stella, *Biochim. Biophys. Acta*, 2013, **1828**, 1013–1024; (b) E. Gatto, G. Bocchinfuso, A. Palleschi, S. Oncea, M. De Zotti, F. Formaggio, C. Toniolo and M. Venanzi, *Chem. Biodivers.,* 2013, **10**, 887-903; (c) M. Crisma, A. Barazza, F. Formaggio, B. Kaptein, Q.B. Broxterman, J. Kamphuis and C. Toniolo, *Tetrahedron*, 2001, **57**, 2813-2825.
4. (a) E. Gazit, I. R. Miller, P. C. Biggin, M. S. P. Sansom and Y. Shai *J. Mol. Biol*., 1996, **258**, 860–870; (b) K. Matsuzaki, O. Murase, H. Tokuda, S. Funakoshi, N. Fujii and K. Miyajima, *Biochemistry*, 1994, **33**, 3342–3349; (c) S. J. Ludtke, K. He, W. T. Heller, T. A. Harroun, L. Yang and H. W. Huang, *Biochemistry*, 1996, **35**, 13723–13728.
5. (a) S. Iftemi, M. De Zotti, F. Formaggio, C. Toniolo, L. Stella and T. Luchian, *Chem. Biodivers.,* 2014, **11**, 1069-1077; (b) G. Bocchinfuso, A. Palleschi, B. Orioni, G. Grande, F. Formaggio, C. Toniolo, Y. Park, K.-S. Hahm and L. Stella, *J. Pept. Sci*., 2009, **15**, 550–558.
6. K. Matsuzaki, *Acc. Chem. Res*., 2014, **47**, 2397–2404.
7. J. R. Brender, S. Salamekh and A. Ramamoorthy, *Acc. Chem. Res*., 2012, **45**, 454-462.
8. (a) H. Lin R. Bhatia and R. Lal, *FASEB J*., 2001, **15**, 2433-2444; (b) Y.-J. Zhang, J.-M. Shi, C.-J. Bai, H. Wang, H.-Y. Li, Y. Wu and S.-R. Ji, *J. Biol. Chem*., 2012, **287**, 748–756.
9. (a) T. L. Williams and L. C. Serpell, *FEBS J.* 2011, **278**, 3905–3917; (b) M. Zheng, J. Zhao and J. Zheng, *Soft Matter*, 2014, **10**, 7425-7451; (c) N. B. Last and A. D. Miranker, *Proc. Natl. Acad. Sci. USA*, 2013, **110**, 6382-6387; (d) S. M. Butterfield and H. A. Lashuel, *Angew. Chem. Int. Ed*, 2010, **49**, 5628-5654.
10. (a) J. Venkatraman, S. C. Shankaramma and P. Balaram, *Chem. Rev.,* 2001, **101**, 3131-3152; (b) C. Toniolo, M. Crisma, G. M. Bonora, E. Benedetti, B. Di Blasio, V. Pavone, C. Pedone and A. Santini, *Biopolymers*, 1991, **31**, 129-138.
11. Z. Shenkarev, A. Paramonov, K. D. Nadezhdin, E. V. Bocharov, I. A. Kudelina, D. A. Skladnev, A. A. Tagaev, Z. A. Yakimenko, T. V. Ovchinnikova and A. Arseniev, *Chem. Biodivers*., 2007, **4**, 1219-1242.
12. R. P. Hummel, C. Toniolo and G. Jung, *Angew. Chem. Int. Ed*., 1987, **26**, 1150-1152.
13. (a) J. Clayden, A. Castellanos, J. Solà and G. A. Morris, *Angew. Chem. Int. Ed*., 2009, **48**, 5962-5965; (b) L. Byrne, J. Solà, T. Boddaert, T. Marcelli, R. W. Adams, G. A. Morris and J. Clayden, *Angew. Chem. Int. Ed*., 2014, **53**, 151-155; (c) S. J. Pike, M. De Poli, W. Zawodny, S. J. Webb and J. Clayden, *Org. Biomol. Chem*., 2013, **11**, 3168-3176.
14. U. Orcel, M. De Poli, M. De Zotti and J. Clayden, *Chem. Eur. J.,* 2013, **19**, 16357–16365.
15. S. J. Pike, V. Diemer, J. Raftery, S. J. Webb and J. Clayden*, Chem. Eur. J*., 2014, **20**, 15981–15990.
16. Longer Aib oligomers display much higher activity. A. Bader, J. Clayden, S. L. Cockroft, V. Diemer, J. E. Jones, J. Raftery, J. Sengel, M. I. Wallace and S. J. Webb, *unpublished*.
17. J. Solà, G. A. Morris and J. Clayden, *J. Am. Chem. Soc*., 2011, **133**, 3712-3715.
18. X. Tian, F. Sun, X.-R. Zhou, S.-Z. Luo and L. Chen, *J. Pept. Sci*. 2015, **21**, 530–539.
19. B. Soberats, L. Martínez, E. Sanna, A. Sampedro, C. Rotger and A. Costa, *Chem. Eur. J*., 2012, **18**, 7533-7542.
20. (a) M. Leclercq, A. Collet and J. Jacques, *Tetrahedron*, 1976, **32**, 821-828; (b) O. Wallach, *Justus Liebigs Ann. Chem*., 1895, **286**, 90-143; (c) C. P. Brock, W. B. Schweizer and J. D. Dunitz, *J. Am. Chem. Soc*., 1991, **113**, 9811-9820; (d) Y. Wang and A. M. Chen, *Org. Process Res. Dev*., 2008, **12**, 282–290.
21. M. Iqbal and P. Balaram, *Biopolymers*, 1982, **21**, 1427-1433.
22. S. J. Pike, T. Boddaert, J. Raftery, S. J. Webb and J. Clayden, *New J. Chem*., 2015, **39**, 3288-3294.
23. (a) G. Lautrette, B. Kauffmann, Y. Ferrand, C. Aube, N. Chandramouli, D. Dubreuil and I. Huc, *Angew. Chem. Int. Ed*., 2013, **52**, 11517-11520; (b) M. Kudo, V. Maurizot, H. Masu, A. Tanatani and I. Huc, *Chem. Commun*., **50**, 10090-10093.
24. S. J. Pike, J. Raftery, S. J. Webb and J. Clayden, *Org. Biomol. Chem*., 2014, **12**, 4124-4131.
25. C. A. Hunter and J. K. M. Sanders, *J. Am. Chem. Soc*., 1990, **112**, 5525–5534.
26. C. P. Wilson, C. Boglio, L. Ma, S. L. Cockroft and S. J. Webb, *Chem. Eur. J*., 2011, **17**, 3465-3473.
27. V. Gorteau, G. Bollot, J. Mareda and S. Matile, *Org. Biomol. Chem*., 2007, **5**, 3000–3012.
28. U. Devi, J. R. D. Brown, A. Almond and S. J. Webb, *Langmuir*, 2011, **27**, 1448-1456.
29. Preliminary planar bilayer conductance (PBC) measurements with micromolar concentrations of the racemic peptides did not show discrete conductance events consistent with stable channels, with the peptides destabilising suspended bilayers instead.
30. "Leaky" fusion of vesicles is unlikely to cause the observed ion transport, as **1** and **2** lack the intermembrane adhesive functionality needed for membrane fusion. See: S. J. Webb, L. Trembleau, R. J. Mart and X. Wang, *Org. Biomol. Chem*. 2005, **3**, 3615-3617.
31. S. R. Durell, H. R. Guy, N. Arispe, E. Rojas and H. B. Pollard, *Biophys. J*., 1994, **67**, 2137-2145.
32. Diasteromeric interactions between the phospholipids/cholesterol in the bilayer and the (*R*) or (*S*) enantiomers are unlikely to measurably alter ionophoric activities. See the ESI.

